



Search for pentaquarks at Belle

K. Abe,¹⁰ K. Abe,⁴⁶ N. Abe,⁴⁹ I. Adachi,¹⁰ H. Aihara,⁴⁸ M. Akatsu,²⁴ Y. Asano,⁵³
 T. Aso,⁵² V. Aulchenko,² T. Aushev,¹⁴ T. Aziz,⁴⁴ S. Bahinipati,⁶ A. M. Bakich,⁴³
 Y. Ban,³⁶ M. Barbero,⁹ A. Bay,²⁰ I. Bedny,² U. Bitenc,¹⁵ I. Bizjak,¹⁵ S. Blyth,²⁹
 A. Bondar,² A. Bozek,³⁰ M. Bračko,^{22, 15} J. Brodzicka,³⁰ T. E. Browder,⁹ M.-C. Chang,²⁹
 P. Chang,²⁹ Y. Chao,²⁹ A. Chen,²⁶ K.-F. Chen,²⁹ W. T. Chen,²⁶ B. G. Cheon,⁴
 R. Chistov,¹⁴ S.-K. Choi,⁸ Y. Choi,⁴² Y. K. Choi,⁴² A. Chuvikov,³⁷ S. Cole,⁴³
 M. Danilov,¹⁴ M. Dash,⁵⁵ L. Y. Dong,¹² R. Dowd,²³ J. Dragic,²³ A. Drutskoy,⁶
 S. Eidelman,² Y. Enari,²⁴ D. Epifanov,² C. W. Everton,²³ F. Fang,⁹ S. Fratina,¹⁵
 H. Fujii,¹⁰ N. Gabyshev,² A. Garmash,³⁷ T. Gershon,¹⁰ A. Go,²⁶ G. Gokhroo,⁴⁴
 B. Golob,^{21, 15} M. Grosse Perdekamp,³⁸ H. Guler,⁹ J. Haba,¹⁰ F. Handa,⁴⁷ K. Hara,¹⁰
 T. Hara,³⁴ N. C. Hastings,¹⁰ K. Hasuko,³⁸ K. Hayasaka,²⁴ H. Hayashii,²⁵ M. Hazumi,¹⁰
 E. M. Heenan,²³ I. Higuchi,⁴⁷ T. Higuchi,¹⁰ L. Hinz,²⁰ T. Hojo,³⁴ T. Hokuue,²⁴
 Y. Hoshi,⁴⁶ K. Hoshina,⁵¹ S. Hou,²⁶ W.-S. Hou,²⁹ Y. B. Hsiung,²⁹ H.-C. Huang,²⁹
 T. Igaki,²⁴ Y. Igarashi,¹⁰ T. Iijima,²⁴ A. Imoto,²⁵ K. Inami,²⁴ A. Ishikawa,¹⁰ H. Ishino,⁴⁹
 K. Itoh,⁴⁸ R. Itoh,¹⁰ M. Iwamoto,³ M. Iwasaki,⁴⁸ Y. Iwasaki,¹⁰ R. Kagan,¹⁴ H. Kakuno,⁴⁸
 J. H. Kang,⁵⁶ J. S. Kang,¹⁷ P. Kapusta,³⁰ S. U. Kataoka,²⁵ N. Katayama,¹⁰ H. Kawai,³
 H. Kawai,⁴⁸ Y. Kawakami,²⁴ N. Kawamura,¹ T. Kawasaki,³² N. Kent,⁹ H. R. Khan,⁴⁹
 A. Kibayashi,⁴⁹ H. Kichimi,¹⁰ H. J. Kim,¹⁹ H. O. Kim,⁴² Hyunwoo Kim,¹⁷ J. H. Kim,⁴²
 S. K. Kim,⁴¹ T. H. Kim,⁵⁶ K. Kinoshita,⁶ P. Koppenburg,¹⁰ S. Korpar,^{22, 15} P. Križan,^{21, 15}
 P. Krokovny,² R. Kulasiri,⁶ C. C. Kuo,²⁶ H. Kurashiro,⁴⁹ E. Kurihara,³ A. Kusaka,⁴⁸
 A. Kuzmin,² Y.-J. Kwon,⁵⁶ J. S. Lange,⁷ G. Leder,¹³ S. E. Lee,⁴¹ S. H. Lee,⁴¹
 Y.-J. Lee,²⁹ T. Lesiak,³⁰ J. Li,⁴⁰ A. Limosani,²³ S.-W. Lin,²⁹ D. Liventsev,¹⁴
 J. MacNaughton,¹³ G. Majumder,⁴⁴ F. Mandl,¹³ D. Marlow,³⁷ T. Matsuishi,²⁴
 H. Matsumoto,³² S. Matsumoto,⁵ T. Matsumoto,⁵⁰ A. Matyja,³⁰ Y. Mikami,⁴⁷
 W. Mitaroff,¹³ K. Miyabayashi,²⁵ Y. Miyabayashi,²⁴ H. Miyake,³⁴ H. Miyata,³² R. Mizuk,¹⁴
 D. Mohapatra,⁵⁵ G. R. Moloney,²³ G. F. Moorhead,²³ T. Mori,⁴⁹ A. Murakami,³⁹
 T. Nagamine,⁴⁷ Y. Nagasaka,¹¹ T. Nakadaira,⁴⁸ I. Nakamura,¹⁰ E. Nakano,³³ M. Nakao,¹⁰
 H. Nakazawa,¹⁰ Z. Natkaniec,³⁰ K. Neichi,⁴⁶ S. Nishida,¹⁰ O. Nitoh,⁵¹ S. Noguchi,²⁵
 T. Nozaki,¹⁰ A. Ogawa,³⁸ S. Ogawa,⁴⁵ T. Ohshima,²⁴ T. Okabe,²⁴ S. Okuno,¹⁶
 S. L. Olsen,⁹ Y. Onuki,³² W. Ostrowicz,³⁰ H. Ozaki,¹⁰ P. Pakhlov,¹⁴ H. Palka,³⁰
 C. W. Park,⁴² H. Park,¹⁹ K. S. Park,⁴² N. Parslow,⁴³ L. S. Peak,⁴³ M. Pernicka,¹³
 J.-P. Perroud,²⁰ M. Peters,⁹ L. E. Piilonen,⁵⁵ A. Poluektov,² F. J. Ronga,¹⁰ N. Root,²
 M. Rozanska,³⁰ H. Sagawa,¹⁰ M. Saigo,⁴⁷ S. Saitoh,¹⁰ Y. Sakai,¹⁰ H. Sakamoto,¹⁸
 T. R. Sarangi,¹⁰ M. Satapathy,⁵⁴ N. Sato,²⁴ O. Schneider,²⁰ J. Schümann,²⁹ C. Schwanda,¹³
 A. J. Schwartz,⁶ T. Seki,⁵⁰ S. Semenov,¹⁴ K. Senyo,²⁴ Y. Settai,⁵ R. Seuster,⁹
 M. E. Sevior,²³ T. Shibata,³² H. Shibuya,⁴⁵ B. Shwartz,² V. Sidorov,² V. Siegle,³⁸
 J. B. Singh,³⁵ A. Somov,⁶ N. Soni,³⁵ R. Stamen,¹⁰ S. Stanić,^{53,*} M. Starić,¹⁵ A. Sugi,²⁴
 A. Sugiyama,³⁹ K. Sumisawa,³⁴ T. Sumiyoshi,⁵⁰ S. Suzuki,³⁹ S. Y. Suzuki,¹⁰ O. Tajima,¹⁰

F. Takasaki,¹⁰ K. Tamai,¹⁰ N. Tamura,³² K. Tanabe,⁴⁸ M. Tanaka,¹⁰ G. N. Taylor,²³ Y. Teramoto,³³ X. C. Tian,³⁶ S. Tokuda,²⁴ S. N. Tovey,²³ K. Trabelsi,⁹ T. Tsuboyama,¹⁰ T. Tsukamoto,¹⁰ K. Uchida,⁹ S. Uehara,¹⁰ T. Uglov,¹⁴ K. Ueno,²⁹ Y. Unno,³ S. Uno,¹⁰ Y. Ushiroda,¹⁰ G. Varner,⁹ K. E. Varvell,⁴³ S. Villa,²⁰ C. C. Wang,²⁹ C. H. Wang,²⁸ J. G. Wang,⁵⁵ M.-Z. Wang,²⁹ M. Watanabe,³² Y. Watanabe,⁴⁹ L. Widhalm,¹³ Q. L. Xie,¹² B. D. Yabsley,⁵⁵ A. Yamaguchi,⁴⁷ H. Yamamoto,⁴⁷ S. Yamamoto,⁵⁰ T. Yamanaka,³⁴ Y. Yamashita,³¹ M. Yamauchi,¹⁰ Heyoung Yang,⁴¹ P. Yeh,²⁹ J. Ying,³⁶ K. Yoshida,²⁴ Y. Yuan,¹² Y. Yusa,⁴⁷ H. Yuta,¹ S. L. Zang,¹² C. C. Zhang,¹² J. Zhang,¹⁰ L. M. Zhang,⁴⁰ Z. P. Zhang,⁴⁰ V. Zhilich,² T. Ziegler,³⁷ D. Žontar,^{21, 15} and D. Zürcher²⁰

(The Belle Collaboration)

¹*Aomori University, Aomori*

²*Budker Institute of Nuclear Physics, Novosibirsk*

³*Chiba University, Chiba*

⁴*Chonnam National University, Kwangju*

⁵*Chuo University, Tokyo*

⁶*University of Cincinnati, Cincinnati, Ohio 45221*

⁷*University of Frankfurt, Frankfurt*

⁸*Gyeongsang National University, Chinju*

⁹*University of Hawaii, Honolulu, Hawaii 96822*

¹⁰*High Energy Accelerator Research Organization (KEK), Tsukuba*

¹¹*Hiroshima Institute of Technology, Hiroshima*

¹²*Institute of High Energy Physics,*

Chinese Academy of Sciences, Beijing

¹³*Institute of High Energy Physics, Vienna*

¹⁴*Institute for Theoretical and Experimental Physics, Moscow*

¹⁵*J. Stefan Institute, Ljubljana*

¹⁶*Kanagawa University, Yokohama*

¹⁷*Korea University, Seoul*

¹⁸*Kyoto University, Kyoto*

¹⁹*Kyungpook National University, Taegu*

²⁰*Swiss Federal Institute of Technology of Lausanne, EPFL, Lausanne*

²¹*University of Ljubljana, Ljubljana*

²²*University of Maribor, Maribor*

²³*University of Melbourne, Victoria*

²⁴*Nagoya University, Nagoya*

²⁵*Nara Women's University, Nara*

²⁶*National Central University, Chung-li*

²⁷*National Kaohsiung Normal University, Kaohsiung*

²⁸*National United University, Miao Li*

²⁹*Department of Physics, National Taiwan University, Taipei*

³⁰*H. Niewodniczanski Institute of Nuclear Physics, Krakow*

³¹*Nihon Dental College, Niigata*

³²*Niigata University, Niigata*

³³*Osaka City University, Osaka*

³⁴*Osaka University, Osaka*

³⁵*Panjab University, Chandigarh*

³⁶*Peking University, Beijing*
³⁷*Princeton University, Princeton, New Jersey 08545*
³⁸*RIKEN BNL Research Center, Upton, New York 11973*
³⁹*Saga University, Saga*
⁴⁰*University of Science and Technology of China, Hefei*
⁴¹*Seoul National University, Seoul*
⁴²*Sungkyunkwan University, Suwon*
⁴³*University of Sydney, Sydney NSW*
⁴⁴*Tata Institute of Fundamental Research, Bombay*
⁴⁵*Toho University, Funabashi*
⁴⁶*Tohoku Gakuin University, Tagajo*
⁴⁷*Tohoku University, Sendai*
⁴⁸*Department of Physics, University of Tokyo, Tokyo*
⁴⁹*Tokyo Institute of Technology, Tokyo*
⁵⁰*Tokyo Metropolitan University, Tokyo*
⁵¹*Tokyo University of Agriculture and Technology, Tokyo*
⁵²*Toyama National College of Maritime Technology, Toyama*
⁵³*University of Tsukuba, Tsukuba*
⁵⁴*Utkal University, Bhubaneswar*
⁵⁵*Virginia Polytechnic Institute and State University, Blacksburg, Virginia 24061*
⁵⁶*Yonsei University, Seoul*

Abstract

We search for the strange pentaquark Θ^+ using kaon interactions in the material of the Belle detector. No signal is observed in the pK_S final state, while in the pK^- final state we observe $\sim 1.6 \cdot 10^4 \Lambda(1520) \rightarrow pK^-$ decays. We set an upper limit on the ratio of Θ^+ to $\Lambda(1520)$ yields $\sigma(\Theta^+)/\sigma(\Lambda(1520)) < 2\%$ at 90% CL, assuming that the Θ^+ is narrow. We also report on searches for strange and charmed pentaquarks in B meson decays. These results are obtained from a 155 fb^{-1} data sample collected with the Belle detector near the $\Upsilon(4S)$ resonance, at the KEKB asymmetric energy e^+e^- collider.

PACS numbers: 13.25.Hw, 13.75.Jz, 14.20.Jn, 14.20.-c

INTRODUCTION

Until recently, all reported particles could be understood as bound states of three quarks or a quark and an antiquark. QCD predicts also more complicated configurations such as glueballs gg , molecules $q\bar{q}q\bar{q}$ and pentaquarks $qqq\bar{q}\bar{q}$. Recently, observations of the pentaquark $\Theta^+ = uudd\bar{s}$ have been reported in the decay channels K^+n [1] and pK_S [2]. Many experimental groups have confirmed this observation and the isospin 3/2 members of the same pentaquark multiplet have also been observed [3]. Evidence for the charmed pentaquark $\Theta_c^0 = uudd\bar{c}$ has also been seen [4]. The topic attracts enormous theoretical interest. However the existence and properties of pentaquarks remain a mystery. Some experimental groups do not see the pentaquark signals. The non-observing experiments correspond to higher center-of-mass energies. It has been argued [5] that pentaquark production is suppressed in the fragmentation regime at high energies.

Charged and neutral kaons are copiously produced at Belle. We treat kaons as projectiles and the detector material as a target, and search for strange pentaquark *formation*, $KN \rightarrow \Theta^+$, and *production*, $KN \rightarrow \Theta^+X$. The kaon momentum spectrum is soft, with a most probable momentum of only $0.6 \text{ GeV}/c$. Therefore we can search for Θ^+ formation in the low energy region.

We also search for strange and charmed pentaquarks in the decays of B mesons, where the suppression of production observed in s channel e^+e^- collisions [6] may be absent. Studies of B meson decays have proved to be very useful for discoveries of new particles (such as P-wave $c\bar{q}$ states), therefore it is interesting to search for pentaquarks in B decays although no firm theoretical predictions for branching fractions exist.

DETECTOR AND DATA SET

These studies are performed using a data sample of 140 fb^{-1} collected at the $\Upsilon(4S)$ resonance and 15 fb^{-1} at an energy 60 MeV below the resonance. The data were collected with the Belle detector [7] at the KEKB asymmetric energy e^+e^- storage rings [8].

The Belle detector is a large-solid-angle magnetic spectrometer that consists of a three layer silicon vertex detector (SVD), a 50-layer cylindrical drift chamber (CDC), a mosaic of aerogel threshold Cherenkov counters (ACC), a barrel-like array of time-of-flight scintillator counters (TOF), and an array of CsI(Tl) crystals (ECL) located inside a superconducting solenoidal coil that produces a 1.5 T magnetic field. An iron flux return located outside the coil is instrumented to detect muons and K_L mesons (KLM).

The proton, kaon and charged pion candidates are identified based on the dE/dx , TOF and Cherenkov light yield information for each track. K_S candidates are reconstructed via the $\pi^+\pi^-$ decays and must have an invariant mass consistent with the nominal K_S mass. The K_S candidate is further required to have a displaced vertex and a momentum direction consistent with the direction from its production to decay vertices.

SEARCH FOR Θ^+ USING KAON INTERACTIONS IN THE DETECTOR MATERIAL.

The analysis is performed by selecting pK^- , pK^+ and pK_S secondary vertices. The protons and kaons are required not to originate from the region around the run-averaged

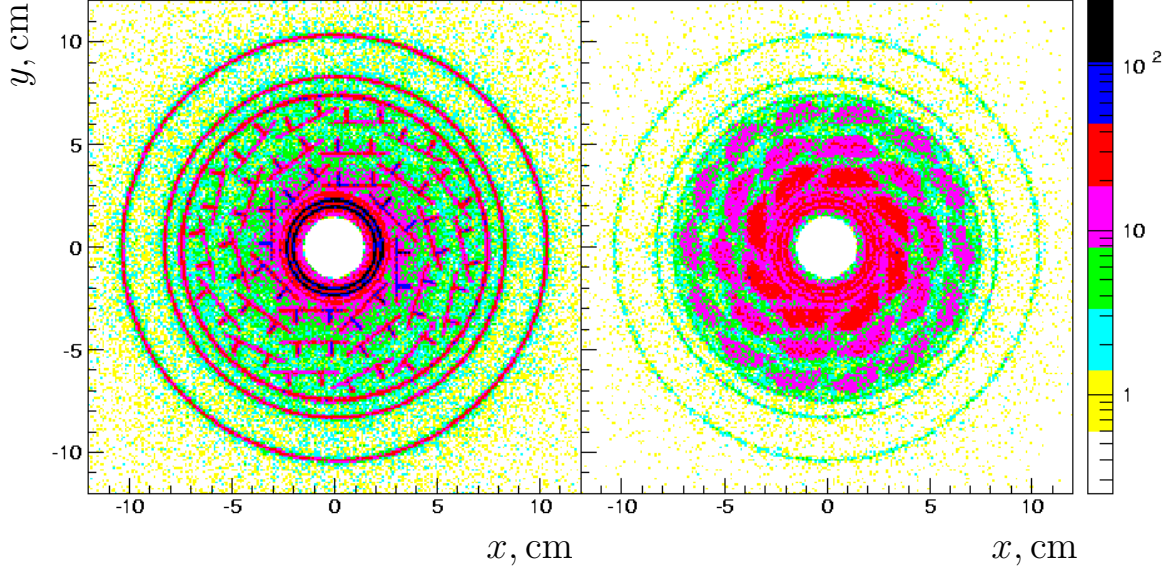


FIG. 1: The xy distribution of secondary pK^- vertices for the barrel (left) and endcap (right) parts of the detector.

interaction point (IP). The proton and kaon candidate are combined and the pK vertex is fitted. The xy distribution of the secondary pK^- vertices is shown in Fig. 1 for the barrel part (left) and for the endcap part (right) of the detector. The double wall beam pipe, three layers of SVD, the SVD cover and the two support cylinders of the CDC are clearly visible. The xy distributions for secondary pK^+ and pK_S vertices are similar.

The mass spectra for pK^- , pK^+ and pK_S secondary vertices are shown in Fig. 2. No significant structures are observed in the $M(pK^+)$ or $M(pK_S)$ spectra, while in the $M(pK^-)$ spectrum a $\Lambda(1520)$ signal is clearly visible. We fit the pK^- mass spectrum to a sum of a

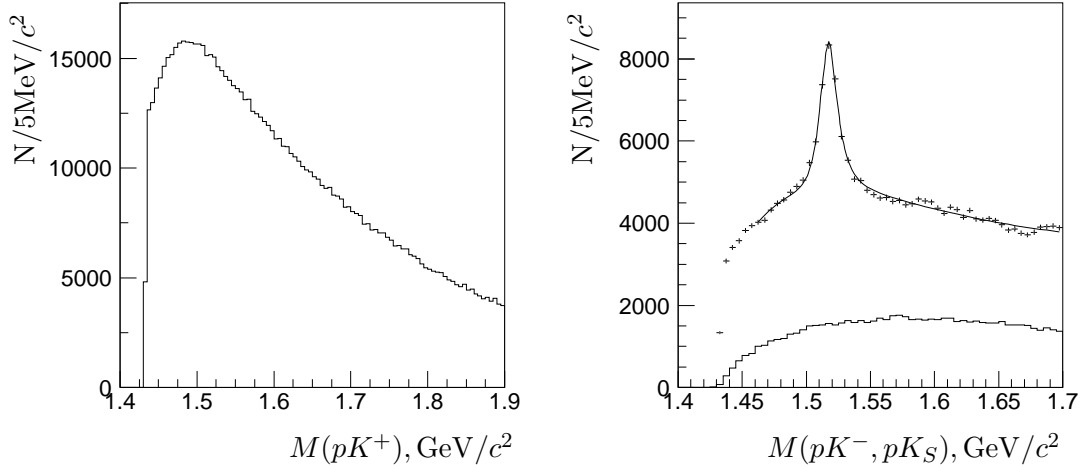


FIG. 2: Mass spectra of pK^+ (left), pK^- (right, points with error bars) and pK_S (right, histogram) secondary pairs. The fit is described in the text.

$\Lambda(1520)$ probability density function (p.d.f.) and a threshold function. The signal p.d.f. is a

D-wave Breit-Wigner shape convolved with a detector resolution function ($\sigma \sim 2 \text{ MeV}/c^2$). The $\Lambda(1520)$ parameters obtained from the fit are consistent with the PDG values [9]. The $\Lambda(1520)$ yield, defined as the signal p.d.f. integral over the $1.48\text{--}1.56 \text{ GeV}/c^2$ mass interval (2.5Γ), is 15519 ± 412 events.

The pK_S mass spectrum is fitted to a sum of a Θ^+ signal p.d.f. and a third order polynomial. The Θ^+ signal shape can be rather complicated because of possible rescattering of particles inside nuclei [10]. In order to compare our result with other experiments we assume that the signal is narrow and its shape is determined by the detector resolution ($\sim 2 \text{ MeV}/c^2$). For $m = 1540 \text{ MeV}/c^2$ the fit result is 29 ± 65 events. Using the Feldman-Cousins method of upper limit evaluation [11] we obtain $N < 94$ events at the 90% CL. We set an upper limit on the ratio of Θ^+ to $\Lambda(1520)$ yields corrected for the efficiency and branching fractions:

$$\frac{N_{\text{observed}}(\Theta^+)}{N_{\text{observed}}(\Lambda(1520))} \frac{\epsilon(pK^-)}{\epsilon(pK_S)} \frac{\mathcal{B}(\Lambda(1520) \rightarrow pK^-)}{\mathcal{B}(\Theta^+ \rightarrow pK_S) \cdot \mathcal{B}(K_S \rightarrow \pi^+\pi^-)} < 2\% \text{ (90\% CL).}$$

It is assumed that $\mathcal{B}(\Theta^+ \rightarrow pK_S) = 25\%$. We take $\mathcal{B}(\Lambda(1520) \rightarrow pK^-) = \frac{1}{2}\mathcal{B}(\Lambda(1520) \rightarrow \bar{N}K) = \frac{1}{2}(45 \pm 1)\%$ [9]. The ratio of efficiencies for $\Theta^+ \rightarrow pK_S$ and $\Lambda(1520) \rightarrow pK^-$ of 37% is obtained from the Monte Carlo (MC) simulation. Our limit is much smaller than the results reported by many experiments which observe Θ^+ . For example it is two orders of magnitude smaller than the value reported by the HERMES Collaboration [13]. We do not know any physical explanation for such a difference.

The momentum spectrum of the produced $\Lambda(1520)$ is shown in Fig. 3 (left). This spectrum

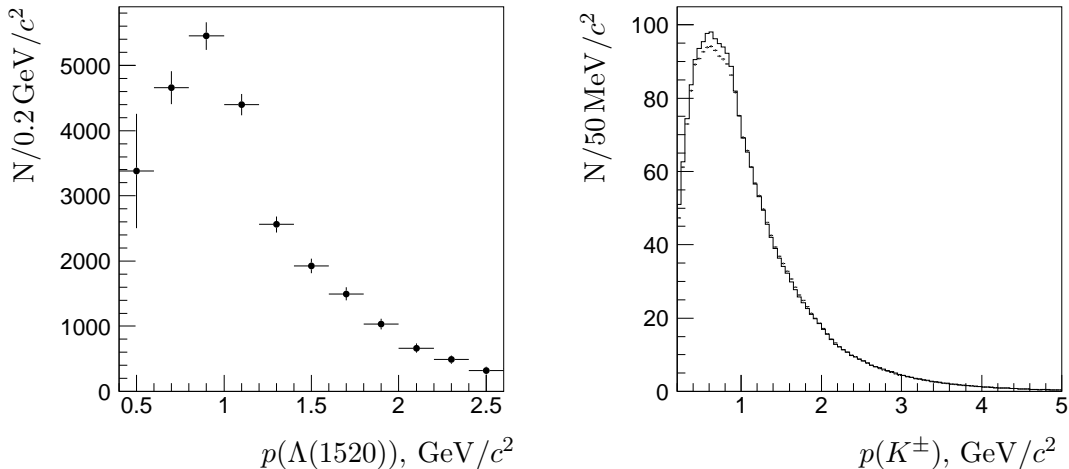


FIG. 3: Left: momentum spectrum of the $\Lambda(1520)$. Right: momentum spectrum of K^- (points with error bars) and K^+ (solid histogram).

is obtained from fitting $M(pK^-)$ in momentum bins and correcting for the efficiency obtained from MC. The K^- should have a $440 \text{ MeV}/c$ momentum to produce $\Lambda(1520)$ on a proton at rest. Even in the presence of Fermi motion with a typical momentum of $150 \text{ MeV}/c$, $\Lambda(1520)$ produced in the *formation* channel should be contained in the first momentum bin, 0.4 to $0.6 \text{ GeV}/c^2$. Therefore most of the $\Lambda(1520)$ are produced in the *production* channel. The projectiles that can produce $\Lambda(1520)$ are K^- , K_S , K_L , Λ . The momentum spectra

of K^- and K^+ are given in Fig. 3 (right). The spectra are corrected for efficiency and for contamination from other particle species. It is not likely that $\Lambda(1520)$ production is dominated by interactions induced by Λ projectiles, because the $\Lambda(1520)$ momentum spectrum is too soft. Even at the threshold of the $\Lambda N \rightarrow \Lambda(1520)p$ reaction the $\Lambda(1520)$ momentum is $\sim 1.1 \text{ GeV}/c$.

To demonstrate that non-strange particles do not produce $\Lambda(1520)$ we study the pK^- vertices accompanied by a K^+ tag. The distance from the pK^- vertex to the nearest K^+ is plotted in Fig. 4 as a dashed histogram. For comparison the distance to any track is plotted as a solid histogram. The peak at zero corresponds to the vertices with additional tracks.

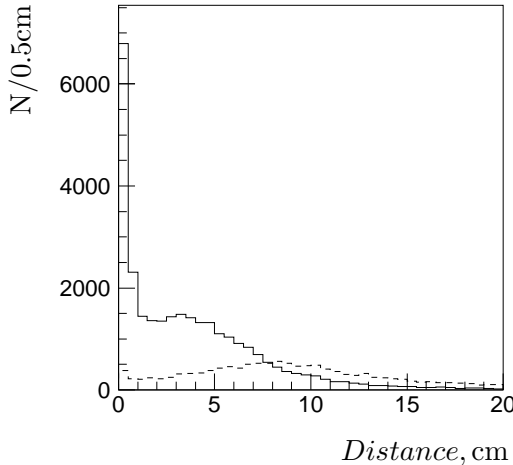


FIG. 4: Distance from pK^- secondary vertex to the nearest track (solid histogram) and to the nearest K^+ (dashed histogram).

The much smaller peak at zero for the K^+ tagged vertices leads us to the conclusion that most $\Lambda(1520)$ are produced by strange projectiles.

SEARCH FOR PENTAQUARKS IN B MESON DECAYS

In this analysis we search for Θ^+ and Θ^{*++} (an isovector pentaquark predicted in some models [12]) in the decays $B^0 \rightarrow \Theta^+ \bar{p}$ followed by $\Theta^+ \rightarrow pK_S$, and $B^+ \rightarrow \Theta^{*++} \bar{p}$ followed by $\Theta^{*++} \rightarrow pK^+$, respectively (inclusion of charge conjugated modes is implied throughout this section). We also search for Θ_c^0 in the decay $B^0 \rightarrow \Theta_c^0 \bar{p}\pi^+$ followed by $\Theta_c^0 \rightarrow D^{(*)-} p$, and Θ_c^{*+} (the charmed analogue of Θ^{*++}) in the decay $B^0 \rightarrow \Theta_c^{*+} \bar{p}$ followed by $\Theta_c^{*+} \rightarrow \bar{D}^0 p$. We reconstruct D mesons in the decay modes $D^{*+} \rightarrow D^0\pi^+$, $D^0 \rightarrow K^-\pi^+$ and $D^- \rightarrow K^-\pi^+\pi^+$. The dominant background arises from the continuum $e^+e^- \rightarrow q\bar{q}$ process. It is suppressed using event shape variables (the continuum events are jet-like, while the $B\bar{B}$ events are spherically symmetric).

The B decays are identified by their CM energy difference, $\Delta E = (\sum_i E_i) - E_{\text{beam}}$, and the beam constrained mass, $M_{\text{bc}} = \sqrt{E_{\text{beam}}^2 - (\sum_i \vec{p}_i)^2}$, where E_{beam} is the beam energy and \vec{p}_i and E_i are the momenta and energies of the decay products of the B meson in the CM frame. The ΔE distribution (with $M_{\text{bc}} > 5.27 \text{ GeV}/c^2$) and M_{bc} distribution (with $|\Delta E| < 0.05 \text{ GeV}/c^2$) for the $B^0 \rightarrow p\bar{p}K_S$ and $B^+ \rightarrow p\bar{p}K^+$ decays are shown in Fig. 5. The

signal yields are extracted by performing unbinned maximum likelihood fits to the sum of signal and background distributions in the two dimensional (M_{bc} , ΔE) space. The signal distributions are determined from MC, whereas the background distributions are determined from the ΔE and M_{bc} sideband data samples. The fits give $28.6^{+6.5}_{-5.8}$ and $216.5^{+17.3}_{-16.6}$ signal

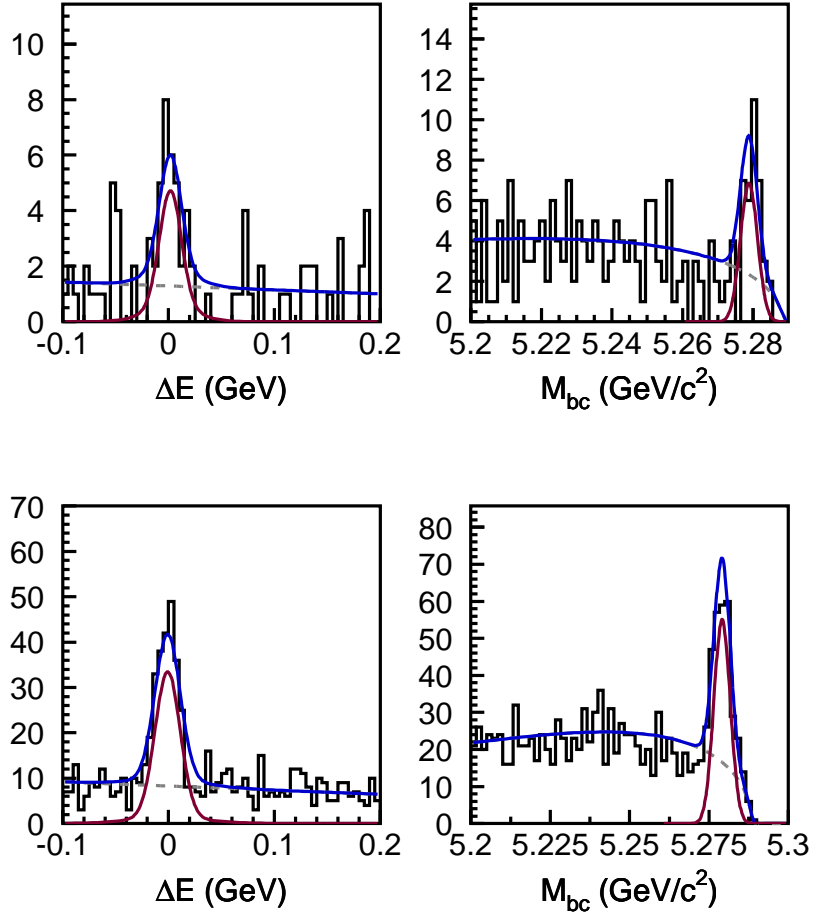


FIG. 5: ΔE and M_{bc} distributions for $p\bar{p}K_S$ (top), and $p\bar{p}K^+$ (bottom) modes. The curves represent the fit results.

yields for the $p\bar{p}K_S$ and $p\bar{p}K^+$ modes, respectively. For the region $1.53 \text{ GeV}/c^2 < M_{pK_S} < 1.55 \text{ GeV}/c^2$, corresponding to the reported Θ^+ mass, we find no signal. Since there is only a theoretical conjecture for the Θ^{*++} , we check the $1.6 \text{ GeV}/c^2 < M_{pK^+} < 1.8 \text{ GeV}/c^2$ region and find no signal. Assuming both states are narrow, we set the upper limits

$$\frac{\mathcal{B}(B^0 \rightarrow \Theta^+ \bar{p}) \times \mathcal{B}(\Theta^+ \rightarrow pK_S)}{\mathcal{B}(B^0 \rightarrow p\bar{p}K_S)} < 22\% \text{ (90\% CL) and}$$

$$\frac{\mathcal{B}(B^+ \rightarrow \Theta^{*++} \bar{p}) \times \mathcal{B}(\Theta^{*++} \rightarrow pK^+)}{\mathcal{B}(B^+ \rightarrow p\bar{p}K^+)} < 2\% \text{ (90\% CL).}$$

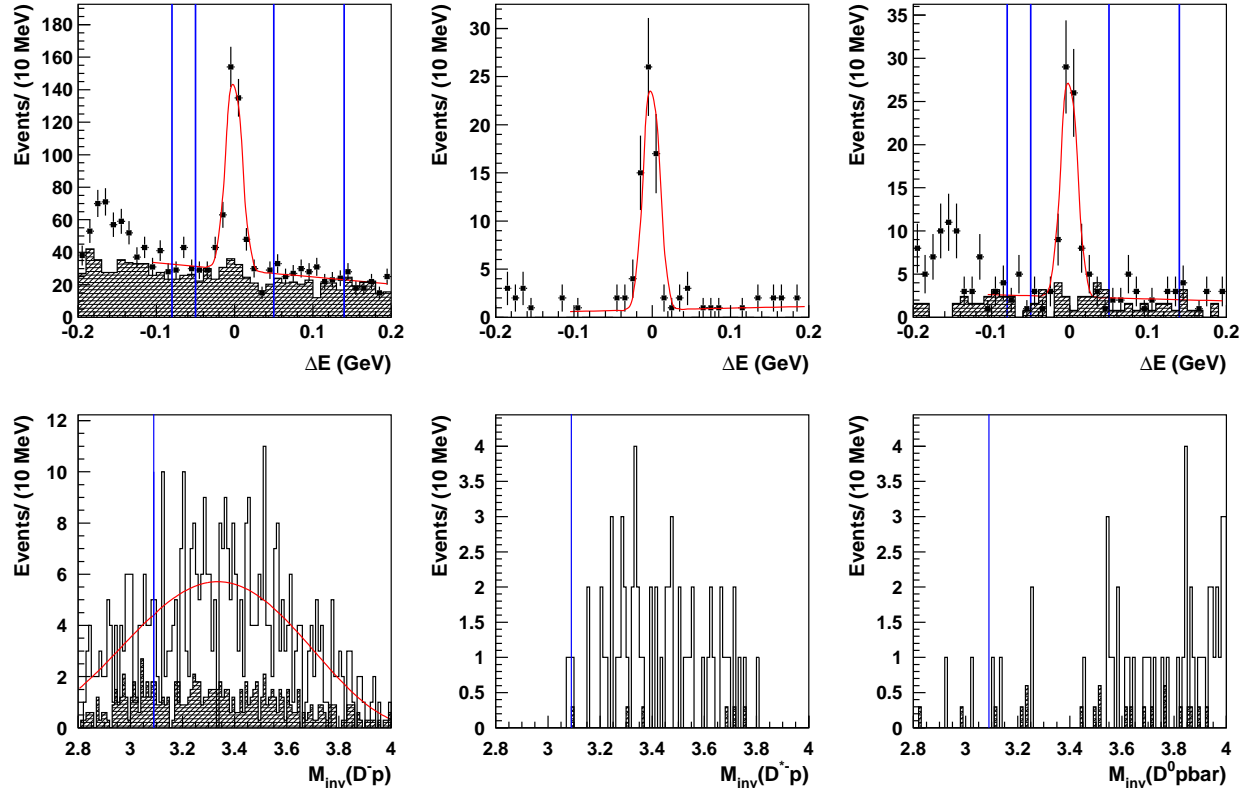


FIG. 6: ΔE and $M(D^{(*)}p)$ distributions for $B^0 \rightarrow D^- p\bar{p}\pi^+$ (left), $B^0 \rightarrow D^{*-} p\bar{p}\pi^+$ (middle) and $\bar{B}^0 \rightarrow D^0 p\bar{p}$ (right) decays. The hatched histogram in ΔE distributions corresponds to the D meson sidebands, while the hatched histogram in $M(D^{(*)}p)$ distributions corresponds to the ΔE sidebands (shown with vertical lines on the ΔE plots). The vertical line in the $M(D^{(*)}p)$ distributions shows the H1 Θ_c^0 mass, $3.099 \text{ GeV}/c^2$.

The ΔE and corresponding $M(D^{(*)}p)$ plots for the decays $B^0 \rightarrow D^- p\bar{p}\pi^+$, $B^0 \rightarrow D^{*-} p\bar{p}\pi^+$ and $\bar{B}^0 \rightarrow D^0 p\bar{p}$ are shown in Fig. 6. From the fit to ΔE spectra the numbers of reconstructed B decays are 303 ± 21 , 60 ± 8 and 66 ± 9 for the three modes, respectively. No signal of Θ_c^0 or Θ_c^{*+} is found in the $M(D^{(*)}p)$ spectra. We set the following upper limits on the fractions of the final state proceeding via Θ_c^0 and Θ_c^{*+} :

$$\begin{aligned} \frac{\mathcal{B}(B^0 \rightarrow \Theta_c^0 \bar{p}\pi^+) \times \mathcal{B}(\Theta_c^0 \rightarrow D^- p)}{\mathcal{B}(B^0 \rightarrow D^- p\bar{p}\pi^+)} &< 1.2\% \text{ (90\% CL)}, \\ \frac{\mathcal{B}(B^0 \rightarrow \Theta_c^0 \bar{p}\pi^+) \times \mathcal{B}(\Theta_c^0 \rightarrow D^{*-} p)}{\mathcal{B}(B^0 \rightarrow D^{*-} p\bar{p}\pi^+)} &< 11\% \text{ (90\% CL)}, \\ \frac{\mathcal{B}(B^0 \rightarrow \Theta_c^{*+} \bar{p}) \times \mathcal{B}(\Theta_c^{*+} \rightarrow \bar{D}^0 p)}{\mathcal{B}(\bar{B}^0 \rightarrow D^0 p\bar{p})} &< 5.9\% \text{ (90\% CL)}. \end{aligned}$$

We assume here that the charmed pentaquark mass is $3.099 \text{ GeV}/c^2$ and that the signal p.d.f. is determined by the detector resolution ($\sim 3.5 \text{ MeV}/c^2$) [4]. Our limits can be compared with the H1 claim that about 1% of D^{*+} mesons originate from Θ_c^0 decays. The branching fraction for Θ_c^0 decays to D mesons is expected to be even larger because of the larger phase

space.

ACKNOWLEDGMENTS

We thank the KEKB group for the excellent operation of the accelerator, the KEK Cryogenics group for the efficient operation of the solenoid, and the KEK computer group and the NII for valuable computing and Super-SINET network support. We acknowledge support from MEXT and JSPS (Japan); ARC and DEST (Australia); NSFC (contract No. 10175071, China); DST (India); the BK21 program of MOEHRD and the CHEP SRC program of KOSEF (Korea); KBN (contract No. 2P03B 01324, Poland); MIST (Russia); MESS (Slovenia); NSC and MOE (Taiwan); and DOE (USA).

* on leave from Nova Gorica Polytechnic, Nova Gorica

- [1] T. Nakano *et al.* (LEPS Collaboration), Phys. Rev. Lett. **91**, 012002 (2003).
- [2] V. Barmin *et al.* (DIANA Collaboration), Phys. Atom. Nucl. **66**, 1715 (2003).
- [3] C. Alt *et al.* (NA49 Collaboration), Phys. Rev. Lett. **92**, 042003 (2004).
- [4] A. Aktas *et al.* (H1 Collaboration), Phys. Lett. **B588**, 17 (2004).
- [5] A. Titov, these Proceedings.
- [6] V. Halyo (BaBar Collaboration), these Proceedings.
- [7] A. Abashian *et al.* (Belle Collaboration), Nucl. Instr. Meth. **A 479**, 117 (2002).
- [8] S. Kurokawa and E. Kikutani, Nucl. Instr. Meth. **A 499**, 1 (2003).
- [9] S. Eidelman *et al.* (Particle Data Group), Phys. Lett. **B592**, 1 (2004).
- [10] A. Sibirtsev *et al.*, nucl-th/0407011.
- [11] G.J. Feldman and R.D. Cousins, Phys. Rev. **D57**, 3873 (1998).
- [12] T. Browder, I. Klebanov and D. Marlow, Phys. Lett. **B587**, 62 (2004).
- [13] A. Airapetian *et al.* (HERMES Collaboration), Phys. Lett. **B585**, 213 (2004).